Journal of Applied Sciences

ISSN 1812-5654

science alert

ANSInet
an open access publisher
http://ansinet.com

Journal of Applied Sciences 8 (4): 574-584, 2008
ISSN 1812-5654

Design and NC Machining of Ball-End Taper Cutter with Constant Pitch

[1]Sheng-Hua Lee, [2]Tian-Syung Lan, [1]Yu-Tang Chen and [3]Wei-Fang Chen
[1]Department of Mechanical Engineering, De Lin Institute of Technology,
Taiwan 236, Republic of China
[2]Department of Information Management, Yu Da College of Business,
Miaoli County, Taiwan 361, Republic of China
[3]Department of Mechanical Engineering, Far East University, Hsin-Shih,
Tainan County 744, Taiwan, Republic of China

Abstract: This study presents the design models of the cutting edge and groove of the ball-end taper cutter with constant pitch. The section profile and relative feeding speeds of the grinding wheel in the NC machining of the cutter are deduced. The problems of remaining revolving surface and no cutting edge strip on the tip part of the ball-end of cutter are post-processed according to the computer simulation result of the actual groove surface. A ball-end taper cutter with ideal grooves may be obtained.

Key words: Ball-end taper cutter with constant pitch, NC machining, reverse engineering of envelope, geometry model

INTRODUCTION

Some problems of helical cutter with constant pitch are discussed in references (Liu, 1998; Tai and Fuh, 1995). The researches are not so deeply and versatile as that on the cutter with constant helical angle, such as references (Liu, 1998; Liu and Liu, 1997, 1998a; Aoyama, 1986; Kataev, 1989; Kaldor *et al*., 1984, 1985; Kang *et al*., 1996; Liu and Liu, 1998b). The researches on the revolving cutter have problems existing at four aspects.

- Only single problem is discussed in most of the references. For example, reference (Liu and Liu, 1998a) only discusses the cutting edge. Reference (Liu and Liu, 1997) only discusses the design of groove. References (Aoyama, 1986; Kataev, 1989; Kaldor *et al*., 1984, 1985; Kang *et al*., 1996) discuss the design of this type of cutter. References (Kang *et al*., 1996; Liu and Liu, 1998a) only discuss the NC machining. Such references are far away from the engineering application. There are still many works need the reader to finish.
- The manufacture cost is high. 3-axis or 4-axis NC machining is adopted in most cases. The rake face of the cutter is machined first; other surfaces are machined gradually (Liu and Liu, 1998a). In this way, one groove is machined in multiple processes, so that the manufacture cost is much higher.
- Planar cutting edge is used in most of the ball-end cutters (Liu and Liu, 1998a; Zhou *et al*., 1991). This is not benefit to the chip removal.
- Continuities of the cutting edge and the feeding speed of grinding wheel at the connecting part are not verified.

Based on the above cases, all the problems (including the design, the NC machining, remedy and post-process) of ball-end taper cutter with constant pitch will be discussed in the study. This is benefit to extension of the equation. These problems are not discussed deeply in references (Liu, 1998) and (Tai and Fuh, 1995). The basic groove is finished mainly in once by 2-axis NC machining so as to decrease the manufacturing cost of cutter. Only about one-seventh of the cutting edge is planar curve at the tip part of the ball-end in the study, this is benefit to the chip removal. The continuities of cutting edge and the feeding speed of grinding wheel along the axial and radial direction will be verified.

The fifth problem in the most references is lack of generality. It is difficult for the research work on certain type of cutter to be extended to the similar cutters. Therefore, this paper will present the general equations first; the detailed equation of the ball-end taper cutter can be deduced from the general equation. The related contents will be discussed as follows.

Corresponding Author: Tian-Syung Lan, Department of Information Management, Yu Da College of Business, Miaoli County, Taiwan 361, Republic of China

THE CONTINUITY OF THE CUTTING EDGE

The revolving surface of special revolving cutter can be expressed by the following general equation:

$$r = \{f(u)\cos\theta, f(u)\sin\theta, g(u)\} \quad (1)$$

For the cutting edge of cutter with a constant pitch, the helical lead is also constant, i.e.,

$$T = 2\pi f(u)\tan\phi \quad (2)$$

is constant. Since f(u) varies with the variation of parameter u, so the angle ϕ between cutting edge and the generator of revolving surface is also the function of u, it is defined by the follows:

$$\tan\phi = \frac{T}{2\pi f(u)} = \frac{b}{f(u)} \quad (3)$$

where, b is the spiral parameter and

$$b = \frac{T}{2\pi} \quad (4)$$

In order to obtain the cutting edge on the surface of Eq. 1, calculate the partial differential of the surface as following:

$$r_u = \{f'(u)\cos\theta, f'(u)\sin\theta, g'(u)\} \quad (5)$$

$$r_\phi = \{-f(u)\sin\theta, f(u)\cos\theta, 0\} \quad (6)$$

The coefficients of first fundamental form is as follows:

$$\begin{cases} E = r_u^2 = f'^2 + g'^2 \\ F = r_u \bullet r_\phi = 0 \\ G = r_\phi^2 = f^2 \end{cases} \quad (7)$$

By use of the definition of angle ϕ between the tangent line dr of cutting edge and the generator δr ($\delta\phi$ = 0) of revolving surface, it is known that:

$$dr = r_u du + r_\theta d\theta \cdot \delta r = r_u \delta u \quad (8)$$

$$\cos^2\phi = (dr \times \delta r)^2 \Big/ \left(|dr|^2 |\delta r|^2\right) \quad (9)$$

Equation 5 can be obtained:

$$\frac{d\theta}{du} = \tan\phi\sqrt{f'^2 + g'^2}\Big/ f = b\sqrt{f'^2 + g'^2}\Big/ f^2 \quad (10)$$

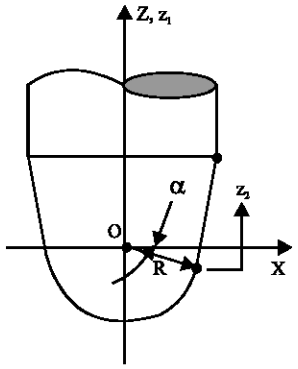

Fig. 1: Ball-end taper cutter

In integration form, Eq. 10 becomes:

$$\theta = b\int_{u_0}^{u} \frac{\sqrt{f'^2 + g'^2}}{f^2} du + \theta_0 \quad (11)$$

where, θ_0 is the initial value of parameter θ, it is defined according to the detailed condition.

It is obvious that the equation of cutting edge with a variable helical angle ψ and constant pitch T may be obtained by substituting Eq. 11 and 1.

For ball-end taper cutter, there are helical cutting edges on the taper part of the cutter. The cutting edge can also be defined by use of Eq. 1 and 11. As shown in Fig. 1, the equation of the sphere is as follows:

$$r_1 = \left\{\sqrt{R^2 - z_1^2}\cos\theta_1, \sqrt{R^2 - z_1^2}\sin\theta_1, z_1\right\} \quad (12)$$

Where:

R = Radius of the sphere
θ_1 = Angular parameter and $\theta_1 \in [0, 2\pi]$
z_1 = Parametric variable and $z_1 \in [-R, -R\sin\alpha]$

Corresponding to Eq. 12 and 1, we have:

$$f = \sqrt{R^2 - z_1^2}, \quad \sqrt{f'^2 + g'^2} = \frac{R}{\sqrt{R^2 - z_1^2}} \quad (13)$$

Corresponding to Eq. 10, we can obtain that:

$$d\theta_1 = \frac{bR}{\left(R^2 - z_1^2\right)^{3/2}} dz_1 \quad (14)$$

After integration, Eq. 12 becomes as follows:

$$\theta_1 = bR\int_0^{z_1} \frac{dz_1}{\left(R^2 - z_1^2\right)^{3/2}} = \frac{bz_1}{R\sqrt{\left(R^2 - z_1^2\right)}} \quad (15)$$

This is because that the initial $\theta_1 = 0$ when $z_1 = 0$, so $\theta_0 = 0$, Eq. 15 may be obtained. At the conjunction position, substitute $z_1 = R \sin \alpha$ into Eq. 15, we have:

$$\theta_{10} = \frac{bz_1}{R\sqrt{(R^2 - z_1^2)}} = -\frac{b}{R}\tan\alpha \tag{16}$$

By referring to Fig. 1, the equation of cone may be expressed as:

$$r_2 = \begin{Bmatrix} (R\cos\alpha + z_2\tan\alpha)\cos\theta_2, \\ (R\cos\alpha + z_2\tan\alpha)\sin\theta_2, (z_2 - R\sin\alpha) \end{Bmatrix} \tag{17}$$

where $z_2 \in [0,h]$
Accordingly, we can get

$$f = R\cos\alpha + z_2\tan\alpha, \quad \sqrt{f'^2 + g'^2} = \sec\alpha \tag{18}$$

Corresponding to Eq. 10, it is known that

$$d\theta_2 = \frac{b\sec\alpha}{(R\cos\alpha + z_2\tan\alpha)^2}dz_2 \tag{19}$$

After integration, we have

$$\theta_2 = \int_0^{z_2} \frac{b\sec\alpha}{(R\cos\alpha + z_2\tan\alpha)^2}dz_2 + \theta_{20} \tag{20}$$

Substitute the boundary condition that $z_2 = 0$ and $\theta_2 = \theta_{20} = \theta_{10}$ into the above equation, we can obtain that:

$$\theta_2 = \int_0^{z_2} \frac{b\sec\alpha}{(R\cos\alpha + z_2\tan\alpha)^2}dz_2 - \frac{b}{R}\tan\alpha \tag{21}$$

By substituting Eq. 21 into Eq. 17 and 16 into Eq. 12, the helical angle of the ball-end taper cutter may be obtained. The helical angle is variable but the pitch is constant.

The actual cutting edge is determined according to the section and relative speeds of grinding wheel in the NC machining. These problems will be introduced as follows.

DEFINITION OF GROOVE SHAPE AND THE EQUATION OF SPIRAL GROOVE

Figure 2 shows the groove section of the cylindrical part and the section plane of the ball-end passing through the center of the ball. The whole section consists of 5 segments. The first segment is a straight line AB, which is the rake face with an rake angle γ. The second segment is arc BC, which helps chip coiling. The third segment is

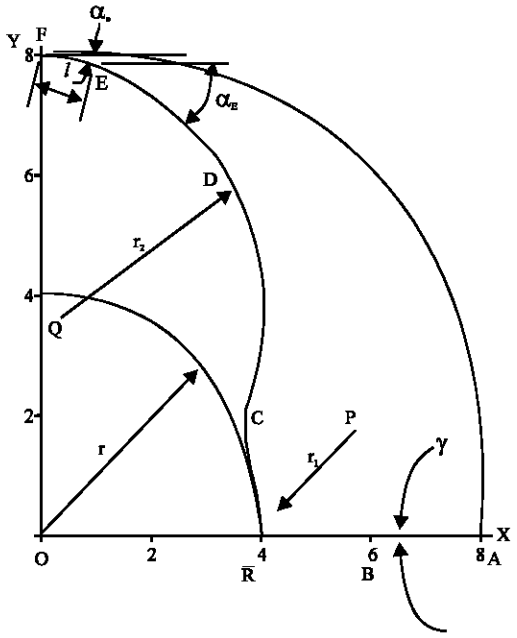

Fig. 2: Sectional shape of the groove

arc CD, which provides adequate strength for the cutter and a smooth path for the chip flow. The fourth segment is straight line DE, which links with the cutting edge land. The cutting edge land designated as the fifth segment is also represented by a straight line EF. Since the radius of the cutter at the ball-end decreases with increasing z-coordinate, the depth of the groove should also gradually decrease accordingly. Therefore, on the ball-end the groove shape needs to be modified. Only part of the five segments will be included, possibly with only section BC remaining. The groove on the cylindrical part is formed by the continuous spiral motion of the above section. The groove on the ball-end part is formed by the enveloping surface of the disc-shaped grinding wheel, which moves at variable radial speed and axial speed and constant rotational speed. The profile of grinding wheel is defined by solving the reverse problem of finding the profile envelope fitting the above groove section.

The groove section as shown in Fig. 2 is for a cutter of four flutes. If the cutter consists of n grooves, the dividing angle of each groove will be 360°/n. In this study, a cutter with four grooves is taken as an example, so the dividing angle of the groove section should be 90°. Let the inner radius of the cylindrical part be r, with rake angle γ, the equation of straight line AB may be defined as:

$$r_{AB} = \left\{\bar{R}, 0\right\} + \lambda_1\{\cos\gamma, \sin\gamma\} = \{x_{AB}, y_{AB}\} \tag{22}$$

where, $\bar{R}$ is the outer radius of cross section.

In order to define the coordinate of point B, the coordinate of center point Q of the arc BC should be calculated first. If the radius of arc BC is r_1, then Q is on the line paralleling to the straight line AB and with a distance r_1. Q is also on the circle centered at point O with radius $r + r_1$. In this way, the coordinate of point Q may be defined by the following equations:

$$\begin{cases} r_Q = r_{A'B'} = \left\{\bar{R} - r\sin\gamma, r\cos\gamma\right\} + \lambda_1\{\cos\gamma, \sin\gamma\} \\ r_Q = r_o = \{(r + r_1)\sin\phi_2, (r + r_1)\cos\phi_2\} \end{cases} \quad (23)$$

where, $\bar{R}$ is the radius of the outer circle, r is the radius of the inner circle, r_1 is the radius of arc BC, γ is the angle between X-axis and segment AB and λ_1 is the length parameter to describe any arbitrary point P on segment AB. The coordinate (x_Q, y_Q) can be calculated after λ_1 and ϕ_2 are solved from (23). The equation of arc BC may be defined as:

$$\begin{cases} x_{BC} = x_Q + r_1\cos\phi_1 \\ y_{BC} = y_Q + r_1\sin\phi_1 \end{cases} \quad (24)$$

Since the arc BC is tangent to straight line AB at point B, the coordinate of point B may be defined as:

$$\begin{cases} x_{AB} = x_{BC} \\ y_{AB} = y_{BC} \end{cases} \quad (25)$$

By substituting Eq. 22 and 24 into Eq. 25, λ_1 and ϕ_2 can be computed. The coordinate of point B can be then be estimated by the equation of 22 or 24. Since the coordinate of point F is $(0, \bar{R})$ and the clearance angle of cutting strip is α_e, the equation of straight line EF can be expressed as:

$$r_{EF} = \left\{0, \bar{R}\right\} + \lambda_2\{\cos\alpha_e, -\sin\alpha_e\} \quad (26)$$

where, λ_2 is the length parameter for describing any arbitrary point on segment EF and α_e is the angle between X-axis and segment EF at point F. The coordinate of point E may be defined by the length l of line EF as:

$$r_E = \left\{l\cos\alpha_e, \bar{R} - l\sin\alpha_e\right\} \quad (27)$$

Let straight line DE is at an angle α_E to x-axis, the equation of straight line DE can be obtained as:

$$r_{DE} = \left\{l\cos\alpha_e, \bar{R} - l\sin\alpha_e\right\} + \mu_1\{\cos\alpha_E, -\sin\alpha_E\} \quad (28)$$

where, μ_1 is the length parameter for describing any arbitrary point on segment DE. In order to satisfy the requirement of cutter strength and smooth chip flow, let the radius of arc CD be r_2. The center P of arc CD is on the line paralleling to the straight line DE at a distance r_2. P is also on the circle, which is centered at point Q and with a radius of $r + r_2$. This is because arc BC is tangent to arc CD at point C and the tangent point C is on the line PQ. In this way, the coordinate of point P may be defined by the above two conditions, i.e.,

$$\begin{cases} r_P = \{x_Q + (r_1 + r_2)\cos\phi_1, y_Q + (r_1 + r_2)\sin\phi_1\} \\ r_P = \left\{l\cos\alpha_e - r_2\sin\alpha_E, \bar{R}\sin\alpha_e - r_2\cos\alpha_E\right\} \\ \qquad + \mu_2\{\cos\alpha_E - \sin\alpha_E\} \end{cases} \quad (29)$$

where, ϕ_1 and μ_2 can be computed by the above equation. The coordinate of point P can also be defined accordingly. Therefore, the equation of arc CD can be expressed as:

$$r_{CD} = \{x_P + r_2\sin\phi_2, y_P + r_2\cos\phi_2\} \quad (30)$$

The coordinate of the tangent point C between arcs BC and CD are given as:

$$\begin{cases} r_{BC} = \{x_Q + r_1\cos\psi, y_Q + r_1\sin\psi\} \\ r_{CD} = \{x_P + r_2\sin\phi_2, y_P + r_2\cos\phi_2\} \end{cases} \quad (31)$$

After solving for ψ and ϕ_2 from the above equations, the coordinate of point C can be obtained from Eq. 31. Since the straight line of DE is tangent to the arc CD at point D, the coordinate of point D can be obtained as:

$$\begin{cases} r_{CD} = \{x_P + r_2\sin\phi_2, y_P + r_2\cos\phi_2\} \\ r_{DE} = \{l\cos\alpha_e, \bar{R} - l\sin\alpha_e\} + \mu_1\{\cos\alpha_E, -\sin\alpha_E\} \end{cases} \quad (32)$$

where, μ_1 and ϕ_2 can be computed from the above equations. The coordinate of point D can then be estimated accordingly. Since the equation for each segment of the groove section is defined, the coordinates of the starting point, connecting points and end points are also obtained, the curves of the groove can now be expressed as:

$$r = \{x(t), y(t)\} = \begin{cases} \{\bar{R} + \lambda\cos\gamma, \lambda\sin\gamma\} = r_{AB} \\ \{x_Q + r_1\cos\psi\ , y_Q + r_1\sin\psi\} = r_{BC} \\ \{x_P + r_2\sin\phi_2, y_P + r_2\cos\phi_2\} = r_{CD} \\ \{l\cos\alpha_e + \mu_1\cos\alpha_E, \bar{R} - l\sin\alpha_e - \mu_1\sin\alpha_E\} = r_{DE} \\ \{\lambda_1\cos\alpha_e, \bar{R} - \lambda_1\sin\alpha_e\} = r_{EF} \end{cases} \quad (33)$$

If the groove is moving along the helical curve on cylindrical surface of the cutter, the equation of the helical groove can be obtained as:

$$r^* = \{x^*, y^*, z^*\} = \begin{Bmatrix} x(t)\cos\bar{\theta} - y(t)\sin\bar{\theta}, \\ x(t)\sin\bar{\theta} + y(t)\cos\bar{\theta}, b\bar{\theta} \end{Bmatrix} \quad (34)$$

where, b is the pitch of the spatial helical curve and can be expressed as:

$$b = R\cot\phi \quad (35)$$

DESIGN FOR THE SECTION PROFILE OF THE GRINDING WHEEL

A new coordinate system $\sigma_1 = [o_1;x_1,y_1,z_1]$ is attached to the grinding wheel, as shown in Fig. 3. Here, the x_1 axis lies on the xoy plane having an angle of 30° counted from the axis x. O_1 is defined by the rake angle γ and arc bc. The centerline axis of the grinding wheel lies on the z_1 axis passing through o_1. Here, o_1z_1 and oz are straight lines on different planes and o_1o is the common normal line. The equation of o_1z_1 in coordinate system σ can be expressed as:

$$r_{z_1} = \left\{\frac{\sqrt{3}}{2}a,\ \frac{a}{2},\ 0\right\} + \mu_3\left\{\frac{\cos\phi}{2},\ -\frac{\sqrt{3}\cos\phi}{2},\ \sin\phi\right\} \quad (36)$$

where, ϕ is the helical angle and a is the distance between the origins O and O_1 of both $\sigma = [O:X,Y,Z]$ and $\sigma_1 = [O_1;X_1,Y_1,Z_1]$ coordinate systems. Since the profile of grinding wheel is a revolving surface, the normal vector of any point on the surface passes through the revolving axis z_1. Therefore, in order to satisfy the condition that every point on the groove surface is a common tangent point of grinding wheel profile and the groove surface, the normal vector of this point passes through the centerline axis of the grinding wheel. That can be expressed as:

$$r_{z_1} = r_\phi = r^* + ?_3 r_t^* \times r_{\bar{\gamma}}^* = \{x^* + \lambda_3 N_X^*, y^* + \lambda_3 N_y^*, z^* + \lambda_3 N_z^*\} \quad (37)$$

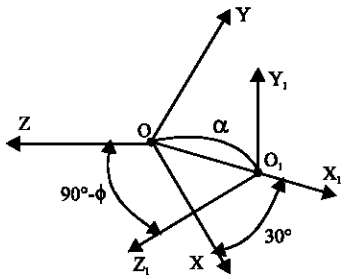

Fig. 3: Relative coordinate systems of σ and σ_1

By equating three components respectively to obtain

$$\frac{\sqrt{3}}{2}a + \mu_3\frac{\cos\phi}{2} = x^* + \lambda_3 N_x^* \quad (38)$$

$$\frac{a}{2} - \mu_3\frac{\sqrt{3}\cos\phi}{2} = y^* + \lambda_3 N_y^* \quad (39)$$

$$\mu_3\sin\phi = z^* + \lambda_3 N_z^* \quad (40)$$

From Eq. 40, one can easily obtain the parameter μ_2 as:

$$\mu_3 = z^*\csc\phi + \lambda_3 N_z^*\csc\phi \quad (41)$$

By substituting the above equation into Eq. 39, the parameter λ_3 is given as:

$$\lambda_3 = \frac{a - \sqrt{3}z^*\cot\phi - 2y^*}{2N_y^* + \sqrt{3}N_z^*\cot\phi} \quad (42)$$

After substituting the above two equations into Eq. 38, the relation can be obtained as:

$$\begin{aligned} &Z^*\cot\phi(N_y^* + \sqrt{3}N_x^*) - N_z^*\cot\phi(\sqrt{3}x^* + y^*) + \\ &a(2N_z^*\cot\phi + \sqrt{3}N_y^* - N_x^*) + 2(y^*N_x^* - x^*N_y^*) = 0 \end{aligned} \quad (43)$$

By using the property of spiral surface, $y^*N_x^* - x^*N_y^* = bN_z^*$, the above relation becomes:

$$\begin{aligned} &Z^*\cot\phi(N_y^* + \sqrt{3}N_x^*) - N_z^*\cot\phi(\sqrt{3}x^* + y^*) \\ &+2bN_z^* + a(2N_x^*\cot\phi + \sqrt{3}N_y^* - N_x^*) = 0 \end{aligned} \quad (44)$$

By simultaneously solving Eq. 34 and 44, the contact curve between the profile of the grinding wheel and the spiral groove may be obtained as:

$$r_j = \{x(\bar{\theta}), y(\bar{\theta}), z(\bar{\theta})\} \quad (45)$$

In order to obtain the profile of the grinding wheel, the above equation of the contact curve is transformed to the coordinate system σ_1, which is attached on the grinding wheel. In order to do so, a new coordinate system $\sigma' = \lfloor o_1; x_1, y', z \rfloor$ is introduced. The transformation from coordinate system σ to coordinate system σ' is given as:

$$\begin{cases} x' = \dfrac{x}{2} + \dfrac{\sqrt{3}}{2} y \\ y' = -\dfrac{\sqrt{3}}{2} x + \dfrac{y}{2} \\ z' = z \end{cases} \tag{46}$$

Since the origin o_1 and both of x_1 and z_1 axes in coordinate system σ_1 are already defined, the direction of y_1 axis can be easily obtained by using the right-hand rule. The transformation from coordinate system σ' to coordinate system σ_1 can then be expressed as:

$$\begin{cases} x_1 = x' - a \\ y_1 = y' \sin\phi + z' \cos\phi \\ z_1 = -y' \cos\phi + z' \sin\phi \end{cases} \tag{47}$$

Thus, the equation of the contact curve can now be expressed in terms of σ_1 coordinate system as:

$$\begin{cases} x_1 = \dfrac{x(\bar{\theta})}{2} + \dfrac{\sqrt{3}}{2} y(\bar{\theta}) - a \\ y_1 = \left(-\dfrac{\sqrt{3}}{2} x(\bar{\theta}) + \dfrac{y(\bar{\theta})}{2} \right) \sin\phi + z(\bar{\theta}) \cos\phi \\ z_1 = \left(\dfrac{\sqrt{3}}{2} x(\bar{\theta}) - \dfrac{y(\bar{\theta})}{2} \right) \cos\phi + z(\bar{\theta}) \sin\phi \end{cases} \tag{48}$$

As the contact curve is rotated around the z_1 axis, the profile surface of the grinding wheel can be computed. The intersecting curve between the profile surface and the plane $y_1 = 0$ is the profile curve of the grinding wheel. This curve can be expressed as:

$$r_c = \left\{ \sqrt{x_1^2 + y_1^2}, 0, z_1 \right\} \tag{49}$$

The grinding wheel having the above profile curve automatically yields a desired groove profile as designed in Eq. 33. However, this is not the case for the ball-end portion of the cutter. To achieve better dimensional accuracy at the ball-end, additional refinement operations should be given to control the wheel motion in radial direction.

CONTINUOUS SPEED OF THE GRINDING WHEEL AXIS AT THE DIRECTION OF RADIAL FEED AND AXIS FEED

In order to adopt the two-axis NC machining, let angular speed ω be constant, the speed v_z along the axial direction can be calculated by:

$$v_z = \frac{dz}{dt} = \frac{dg}{dt} = g' \frac{du}{d\phi} \frac{d\phi}{dt} = \frac{\omega f'^2 g'}{b\sqrt{f'^2 + g'^2}} \tag{50}$$

At the ball-end of the cutter, the speed of grinding wheel along the axial direction can be defined as:

$$v_{z_1} = \frac{\omega\left(R^2 - z_1^2\right)^{3/2}}{bR} \tag{51}$$

For the cone surface, the speed of grinding wheel along the axial direction can be defined as:

$$v_{z2} = \frac{dz_2}{dt} = \omega \frac{\left(R\cos\alpha + z_2 \tan\alpha\right)^2}{b\sec\alpha} \tag{52}$$

At the conjunction place, $z_1 = -R\sin\alpha$ for surface (1) and $z_2 = 0$ for surface (17), substitute the above boundary conditions into Eq. 51 and 52, respectively, we have:

$$v_{z1} = \frac{\omega R^2 \cos^3\alpha}{b} = v_{z2} \tag{53}$$

Equation 53 demonstrates that the axial speed in the NC machining of the whole cutter is a continuous function.

The feeding speed of grinding wheel at the radial direction must be defined according to radius function f(u). If the feeding speed varies linearly with the radius, over-cut will happen at the part of $f(u) < \bar{R}$. If the radial feeding speed is neglected, the groove will not exist at the part of radius less than r. The proper feeding amount should think about the general variation $\bar{R}$ of radius and the general variation r of feeding amount. Let the feeding amount S_g vary proportionally to the variation $\bar{R} - f(u)$ of radius, i.e., $S_g / \left(\bar{R} - f(u)\right) = r/\bar{R}$, we can get:

$$S_g = r - \frac{r}{\bar{R}} f(u) \tag{54}$$

Accordingly, the general equation of feeding speed at the radial direction is as follows:

$$v_g = \frac{dS_g}{dt} = -\frac{r}{\bar{R}} f' \frac{du}{d\phi} \frac{d\phi}{dt} = -\frac{r}{b\bar{R}} \frac{\omega f'^2 f'}{\sqrt{f'^2 + g'^2}} \tag{55}$$

At the ball-end of cutter, the radial speed of grinding wheel is as follows:

$$v_{g1} = \frac{\omega r z_1 \left(R^2 - z_1^2\right)}{bR\bar{R}} \tag{56}$$

For the cone surface, the speed of radial motion can be defined as:

$$v_{g2} = -\frac{\omega r \sin\alpha \left(R\cos\alpha + z_2 \tan\alpha\right)^2}{b\bar{R}} \tag{57}$$

Substitute the conjunction condition into Eq. 56 and 57, we can get:

$$v_{g1} = v_{g2} = -\frac{\omega r R^2 \sin\alpha \cos^2\alpha}{b\bar{R}} \tag{58}$$

Equation 58 explains that the radial speed of the grinding wheel is a continuity function.

The actual obtained groove on the cutter in the NC machining is defined by the enveloping surface of grinding wheel. The actual obtained groove should be verified by computer simulation.

COMPUTER SIMULATION AND REMEDY

The cutting edge and the section of actual obtained groove are to be simulated by computer. According to the simulation results, the correctness of initial assumptions can be evaluated.

It is obvious that f(u) expresses the radius of section circle for a certain value of u. Use the following equations:

$$\begin{cases} \sqrt{x^{*2} + y^{*2}} = f(u) \\ z^{*} = z(u) = g(u) \\ \left(r_{xc}^{*}, r_v^{*}, r_u^{*}\right) = 0 \end{cases} \tag{59}$$

we can get two intersect points of section circle at the position of $z^* = g(u)$, let the point on the cutting edge be (x_1^*, y_1^*, z_1^*), the other point be (x_2^*, y_2^*, z_2^*). The actual obtained cutting edge is at the outside of designed cutting edge except the tip of ball-end, but the distance is very small and the two cutting edges are approximate offset curve with each other. At the area near the tip of ball-end, over-cut exists. So remedy is necessary.

The actual groove section at position of $z = g(u_0)$ may be obtained by different value of x_c. It is obvious that the cutting edge strip decreases gradually with the decrement of radius. At the tip part of the ball-end, the strip does not exist any more. The remaining revolving surface exists between the adjacent grooves since the

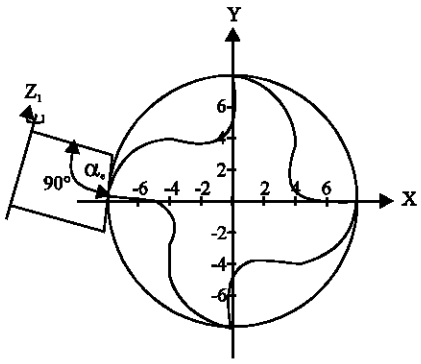

Fig. 4: Relative position between grinding wheel and top of the cutter

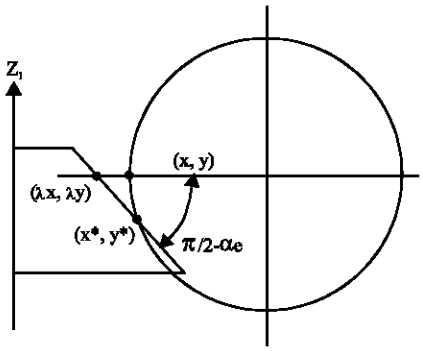

Fig. 5: Define the factor λ

center angle corresponding to each groove is less than 90°. According to the above simulation results, the machining methods at the tip part of the ball-end should be modified so that the over-cut can be diminished.

The radius $rf/\bar{R}$ of groove bottom should be greater than i.e., $\left(\sqrt{2}-1\right)\cdot r_1$

$$rf/\bar{R} \geq \left(\sqrt{2}-1\right)\cdot r_1 \tag{60}$$

i.e.:

$$f \geq \bar{R}\left(\sqrt{2}-1\right)\cdot r_1 / r = r_0 \tag{61}$$

Otherwise, the cutting edge adopts planar curve when $f<r_0$. Examples verify that the planar curve of the cutting edge at the tip of ball-end only takes about one-seventh of the cutting edge at the ball-end of the cutter.

The problem of remaining surface and no strip may be remedied by the following approach. A cone-shaped grinding wheel with a bottom angle of $90°-\alpha_e$ is used to eliminate the remains. The relative position between the grinding wheel and the cutter is as shown in Fig. 4. By means of the relationship between designed point (x., y) and the actual point (x*,y*) on the cutting edge (Fig. 5):

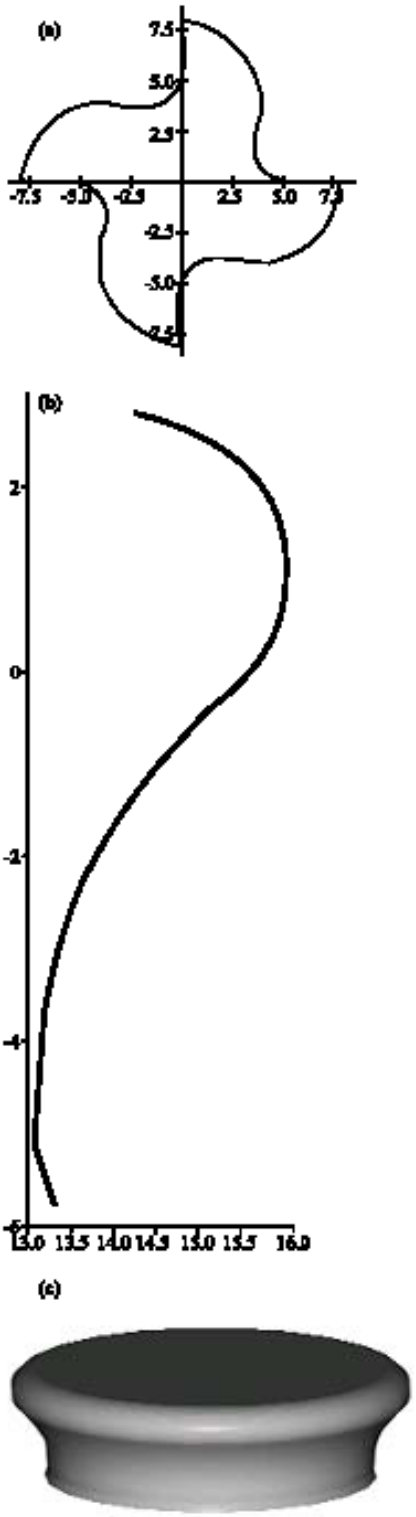

Fig. 6: The grinding wheel and sectional profile. (a) the groove section of the cutter (b) sectional profile of the grinding wheel and (c) the grinding wheel

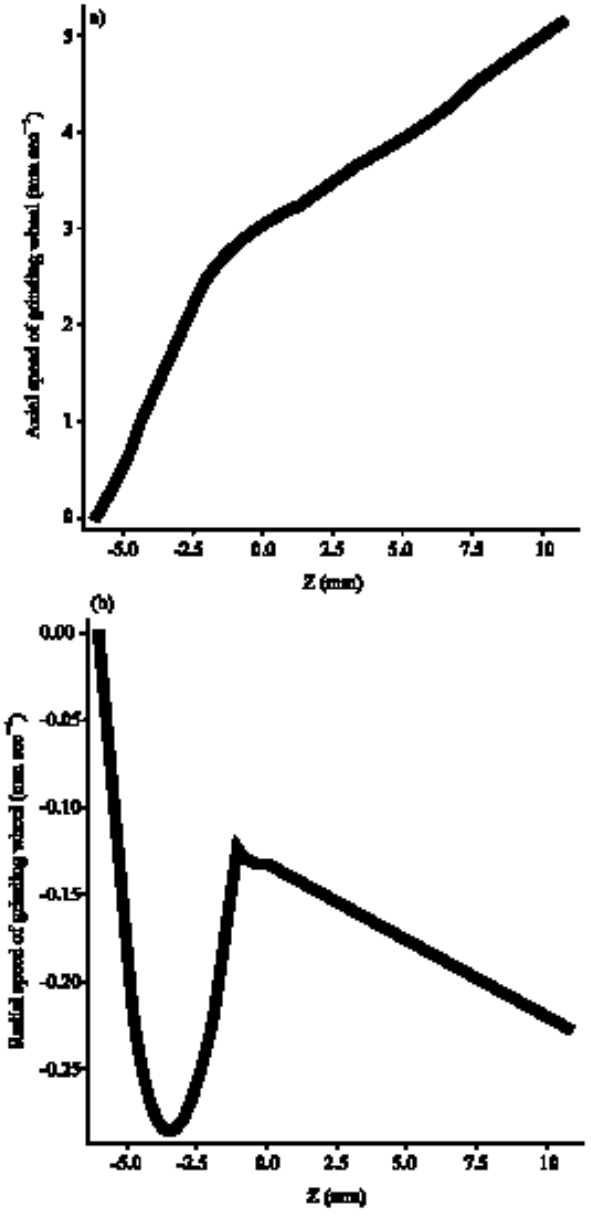

Fig. 7: Feeding speed of the grinder in both the axial and the radial directions. (a) Axial speed of grinding wheel (b) Radial speed of grinding wheel

$$(x,y)\{\lambda x - x^*, \lambda y - y^*\} - \sqrt{x^2+y^2}\sqrt{(\lambda x - x^*)^2 + (\lambda y - y^*)^2}\sin\alpha_c = 0 \quad (62)$$

the factor λ may be defined. Then calculate the revised radial speed by:

$$\overline{v}_c = \frac{d(\lambda f)}{dt} = \frac{d\left(\lambda\sqrt{x^2+y^2}\right)}{dt} \quad (63)$$

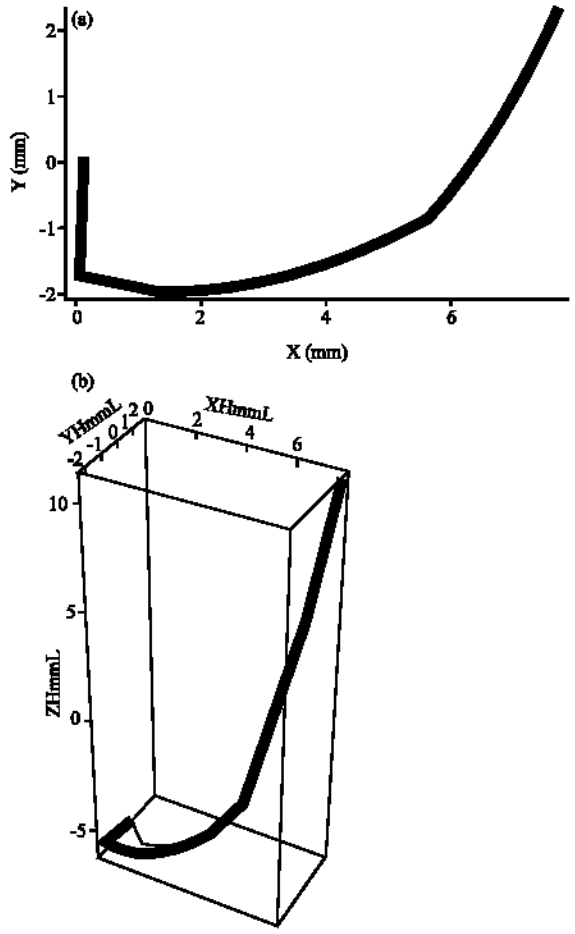

Fig. 8: The desired and actual (dark line) obtained cutting edge curve (dimension: mm) (a) Projected cutting edge curve of the cutter on X-Y plane (b) Spatial cutting edge curve of the cutter

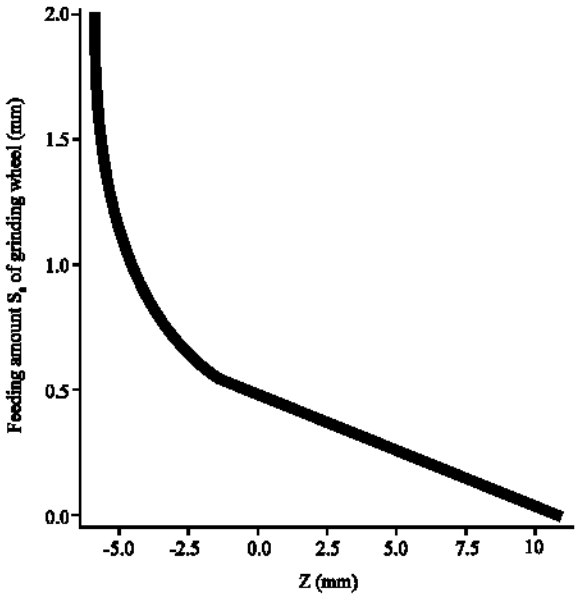

Fig. 9: The feeding amount S_ε of grinding wheel

Fig. 10: Te actual produced ball-end taper milling cutter

Keep axial speed and revolving speed unchanged, replace radial speed v_ε with $\overline{v}_\varepsilon$, the remains revolving surface can be diminished A ideal special revolving cutter may be obtained.

A ball-end taper milling cutter is selected as one example to illustrate the effectiveness of the proposed mathematical modeling and residual compensation method. This cutter possesses a helical angle of $\pi/6$, a rake angle of $\gamma = 5°$, the radius of groove arc BC of $r_1 = 2$ mm, the radius of groove arc CD of $r_2 = 4$ mm, the length of the cutting edge strip of $l = 1$ mm, the clearance angles of cutting strip of $\alpha_e = 6°$ and $\alpha_E = 60°$, cylindrical radius of 8 mm and a taper angle of 10°, a taper height of $h = 11.860$ mm and the remaining circular end radius of 2 mm, $z_1 \in [-6, -1.042]$ mm, $z_1 \in [0, 11.860]$ mm, the distance between the origins O and O_1 of $a = 20$ mm, a spiral parameter of $b = 32/\pi$ mm, a helical lead of $T = 64$ mm. The computed typical sectional profile of the helical groove on the ball-end taper milling cutter is given in Fig. 6a. The grinding wheel and the sectional profile of the grinding wheel are Fig. 6b and c.

Figure 7 shows the feeding speed of the grinder in both the axial and the radial directions. Figure 8 shows the various views of the ball-end taper milling cutter cutting edge curve. Figure 9 shows the feeding amount S_ε of grinding wheel. Figure 10 shows the actual produced ball-end taper milling cutter.

CONCLUSIONS

This study presents a modeling method that can be used to design and manufacture a ball-end taper milling

cutter by using a simple two-axis NC machine. From the related models of design and NC machining and the simulated results, it is known that the general models for the ball-end taper cutter are presented in this study. The validity of machining this kind of cutter by two-axis NC machining is verified by example. The surface shape around the interfacial cross-sectional circle between the spherical head and the taper cone is also derived to ensure the geometric continuity of the model. The instantaneous feed rates in both the axial and the radial directions are also derived based on the rotating speed of the cutter. This study presents ideal method for the design and machining of helical groove of ball-end taper cutter with constant pitch, it is valuable for reference.

ACKNOWLEDGMENT

The authors would like to thank the anonymous referees who kindly provide the suggestions and comments to improve this study.

NOMENCLATURE

a = Distance between the origins O and O_1
b = Spiral parameter
E = Coefficients of first fundamental form ($= r_u^2$)
F = Coefficients of first fundamental form ($= r_u \bullet r_\phi$)
$f(u)$ = Radius function
G = Coefficients of first fundamental form ($= r_\phi^2$)
l = Length of line segment EF
n = number of grooves
R = Radius of the sphere
$\bar{R}$ = Outer radius of groove
r = Equation of the revolving surface of special revolving cutter
r = Inner radius of groove
r_1 = Equation of the sphere
r_1 = Radius of arc BC
r_2 = Equation of the cone
r_2 = Radius of arc CD
r_e = Sectional profile of grinding wheel
r_j = Contact curve between the profile of the grinding wheel and the spiral groove
r^* = Equation of the helical groove
S_g = Radial displacement of grinding wheel
T = Pitch of spiral
v_g = Radial feeding speed of grinding wheel
$\bar{v}_g$ = Actual modified radial feeding speed of grinding wheel
v_z = Axial feeding speed of grinding wheel
z_1, z_2 = Parametric variable of z coordinate
α = Angle of taper
α_e = Clearance angle of cutting strip
α_E = Angle of straight line EF to the X-axis
ϕ = Helical angle
ϕ_1 = Angular parameter of circle
ϕ_2 = Angular parameter of circle
θ = Angular parameter of revolving surface
$\bar{\theta}$ = Angular parameter of revolving surface
θ_0 = Initial value of parameter ϕ
θ_1 = Angular parameter of the sphere
θ_2 = Angular parameter of the cone
γ = Rrake angle of groove
λ = Actual modified radial feeding speed parameter of grinding wheel
λ_1 = Length parameter
λ_2 = Length parameter
λ_3 = Length parameter
μ_1 = Length parameter
μ_2 = Length parameter
μ_3 = Length parameter
ψ = Angular parameter
σ = Coordinate system attached to the pinion cutter
σ_1 = Coordinate system attached to the grinding wheel
σ' = Temporary coordinate system; σ rotates 45° around z-axis
ω = Revolving angular velocity of the cutter

REFERENCES

Aoyama, H.H., 1986. Development of elliptic ball-end mill. Bulls. Jap. Soc. Prec. Eng., 20 (4): 59-66.

Kaldor, S., P.H.H. Trendler and T. Hodgson, 1984. Investigation into the clearance geometry of end mills. Ann. CIRP., 33 (1): 133-139.

Kaldor, S., P.H.H. Trendler and T. Hodgson, 1985. Investigation and optimization of the clearance geometry of end mills. Ann. CIRP., 34 (1): 153-159.

Kang, S.K., K.F. Ehmann and C. Lin, 1996. A CAD approach to helical groove machining mathematical model and model solution. Int. J. Mach. Tools Manuf., 36 (1): 141-153.

Kataev, A.V., 1989. Computer aided design of tool with complex forming faces. Soviet Eng., 9 (7): 22-28.

Liu, J.Y. and H.M. Liu, 1997. Mathematical model of helical flutes of cone milling cutter. Tool. Eng., 4 (2): 3-6.

Liu, J.Y., 1998. Study on geometric modeling and theory about NC machining of special revolving tool. Ph.D Thesis, Harbin Institute of Technology.

Liu, J.Y. and H.M. Liu, 1998a. The general model of helical cutting edge of cutter the common spiral curve. Tool. Eng., 6 (1): 21-23.

Liu, J.Y. and H.M. Liu, 1998b. Geometric model and NC grinding model and computer simulation of ball-end mill with constant normal rake angle. Tool. Eng., 2 (1): 3-5.

Tai, C.C. and K.H. Fuh, 1995. Model for cutting forces prediction in ball-end milling. Int. J. Mach. Tools Manuf., 35 (4): 511-524.

Zhou, C.X., D.Q. Yue and X.T. Wu, 1991. The forming principle of special revolving cutter with planar rake plane. Tool. Eng., 5 (2): 17-21.